Dissipation in Turbulent Flows

J. Christos Vassilicos

Department of Aeronautics, Imperial College London, London SW7 2AZ, United Kingdom; email: j.c.vassilicos@imperial.ac.uk

Annu. Rev. Fluid Mech. 2015. 47:95–114

First published online as a Review in Advance on August 25, 2014

The *Annual Review of Fluid Mechanics* is online at fluid.annualreviews.org

This article's doi: 10.1146/annurev-fluid-010814-014637

Keywords

Richardson-Kolmogorov cascade, nonequilibrium turbulence, turbulence dissipation scalings

Abstract

This article reviews evidence concerning the cornerstone dissipation scaling of turbulence theory: $\epsilon = C_\epsilon \mathcal{U}^3/\mathcal{L}$, with $C_\epsilon = \text{const.}$, ϵ the dissipation rate of turbulent kinetic energy $\mathcal{U}^2$, and $\mathcal{L}$ an integral length scale characterizing the energy-containing turbulent eddies. This scaling is intimately linked to the Richardson-Kolmogorov equilibrium cascade. Accumulating evidence shows that a significant nonequilibrium region exists in various turbulent flows in which the energy spectrum has Kolmogorov's $-5/3$ wave-number scaling over a wide wave-number range, yet $C_\epsilon \sim Re_I^m/Re_L^n$, with $m \approx 1 \approx n$, Re_I a global/inlet Reynolds number, and Re_L a local turbulence Reynolds number.

1. INTRODUCTION

This review begins with quotations from two influential textbooks and one APS Fluid Dynamics Prize presentation. Referring to the well-known estimate $\epsilon \sim \mathcal{U}^3/\mathcal{L}$ (where ϵ is the dissipation rate of turbulent kinetic energy $\mathcal{U}^2$, and $\mathcal{L}$ is the integral length scale), Tennekes & Lumley (1972) stated that this estimate "should not be passed over lightly. It is one of the cornerstone assumptions of turbulence theory." In a paper that Lumley (1992) wrote 20 years later on the occasion of his award of the APS Fluid Dynamics Prize, he included the following question and answer: "What part of modeling is in serious need of work? Foremost, I would say, is the mechanism that sets the level of dissipation in a turbulent flow, particularly in changing circumstances." And in one of the more recent and most widely used textbooks on turbulence, Pope's (2000) chapter "The Scales of Turbulent Motion" begins with a brief description of the Richardson-Kolmogorov cascade that ends "this picture of the cascade indicates that ϵ scales as $\mathcal{U}^3/\mathcal{L}$ independent of ν (at the high Reynolds numbers being considered)," where ν is the fluid's kinematic viscosity.

The one mechanism for turbulence dissipation at high Reynolds numbers that has dominated turbulence textbooks and research activity over the past seven decades is indeed the Richardson-Kolmogorov cascade. Rigid boundaries also introduce their own dissipation mechanism in the case of turbulent flows attached to or affected by a wall. However, the Richardson-Kolmogorov cascade is present (or at least believed to be present) far enough from the wall in many such flows, as in boundary-free turbulent flows, and this review therefore concentrates on the pervasive turbulence dissipation mechanism caused by this cascade. Section 2 briefly reviews this mechanism and its consequences, and Section 3 follows with a review of the experimental evidence gathered in support of $\epsilon \sim \mathcal{U}^3/\mathcal{L}$ in the 50 years after Kolmogorov (1941a,b,c). Section 4 discusses the experimental and computational support for $\epsilon \sim \mathcal{U}^3/\mathcal{L}$ in the past 25 years, and Section 5 reviews the support gathered for a different scaling relation in the past 8 years. Section 6 concludes with a summary and discussion of the new perspectives now opening for research in turbulent flows.

2. THE RICHARDSON-KOLMOGOROV CASCADE

The Richardson-Kolmogorov cascade is a mechanism for turbulence dissipation at high Reynolds numbers when the turbulence is assumed to be at equilibrium (see the chapter "The Universal Equilibrium Theory" in Batchelor 1953; note that the word equilibrium in this chapter and in the present review is not used in the sense reserved in statistical physics for stationary states satisfying detailed balance such as thermal equilibria). The kinetic energy of velocity fluctuations cascades from large to small scales of motion. When it reaches a scale small enough for viscous dissipation to be effective, it dissipates into heat (see Richardson 1922). This cascade is an equilibrium cascade. The rate at which kinetic energy crosses a length scale r where the turbulent fluctuations have a characteristic velocity $u(r)$ is the same from the largest to the smallest length scale r in the appropriate range of scales. This rate can be dimensionally estimated as $u(r)^3/r$ (no viscosity) and can be equated (equilibrium) to the turbulent kinetic energy dissipation $\epsilon = \nu <\mathbf{s}^2>$, where $\mathbf{s}$ is the fluctuating turbulence strain rate tensor, and the brackets signify an appropriate averaging operation. The largest such length scale r is of the order of the integral length scale $\mathcal{L}$ so that $u(r) = u(\mathcal{L}) \sim \mathcal{U}$. Hence, it follows that $\epsilon \sim \mathcal{U}^3/\mathcal{L}$.

These words translate into equations in a way that is based on a relatively recent generalization and use of the Kármán-Howarth equation that is worth recording in this review. Defining $\delta\mathbf{u} \equiv \mathbf{u}(\mathbf{x} + \frac{1}{2}\mathbf{r}, t) - \mathbf{u}(\mathbf{x} - \frac{1}{2}\mathbf{r}, t)$, where $\mathbf{u}$ is the fluctuating velocity field at a given point in space and time, one takes the mathematical definition of $u(r)$ to be $\sqrt{<|\delta\mathbf{u}|^2>}$, which is a function of $\mathbf{x}$ and $\mathbf{r}$. The brackets are an average over time or over statistical realizations of the turbulence. The

Navier-Stokes equation and incompressibility at both $\boldsymbol{\xi} = \boldsymbol{\xi}_+ \equiv \mathbf{x} + \frac{1}{2}\mathbf{r}$ and $\boldsymbol{\xi} = \boldsymbol{\xi}_+ \equiv \mathbf{x} - \frac{1}{2}\mathbf{r}$ are

$$\frac{\partial}{\partial t}(\mathbf{U}+\mathbf{u}) + (\mathbf{U}+\mathbf{u})\cdot\nabla_{\boldsymbol{\xi}}(\mathbf{U}+\mathbf{u}) = -\boldsymbol{\nabla}_{\boldsymbol{\xi}}(P+p) + \nu\boldsymbol{\nabla}^2_{\boldsymbol{\xi}}(\mathbf{U}+\mathbf{u}) \tag{1}$$

and $\boldsymbol{\nabla}_{\boldsymbol{\xi}}\cdot\mathbf{U} = 0$, $\boldsymbol{\nabla}_{\boldsymbol{\xi}}\cdot\mathbf{u} = 0$, where $\mathbf{U}$ is the mean flow field and the Reynolds decomposition $\mathbf{U}+\mathbf{u}$ is used. From these equations written at both points $\boldsymbol{\xi} = \boldsymbol{\xi}_+$ and $\boldsymbol{\xi} = \boldsymbol{\xi}_-$, Hill (2002) and Marati et al. (2004), followed by Danaila et al. (2012) and P. Valente & J.C. Vassilicos (submitted manuscript), derived the generalized Kármán-Howarth equation, which is valid with no homogeneity and no isotropy assumptions:

$$\frac{D^*}{Dt}<|\delta\mathbf{u}|^2> + \boldsymbol{\nabla}_{\mathbf{r}}<(\delta\mathbf{u}+\delta\mathbf{U})|\delta\mathbf{u}|^2> = P^* + T^* + D^* + \nu\boldsymbol{\nabla}^2_{\mathbf{r}}<|\delta u|^2> - 4\epsilon^*, \tag{2}$$

where $D^*/(Dt) \equiv \partial/(\partial t) + \frac{1}{2}[\mathbf{U}(\boldsymbol{\xi}_+) + \mathbf{U}(\boldsymbol{\xi}_-)]\cdot\boldsymbol{\nabla}_x$, and P^*, T^*, and D^* are terms that result from the turbulence production by the mean flow and Reynolds stresses, turbulent transport in terms of gradients in $\mathbf{x}$ space of correlations between velocity fluctuations and both energy and pressure fluctuations, and viscous diffusion in $\mathbf{x}$ space, respectively. The penultimate term on the right-hand side represents viscous diffusion in $\mathbf{r}$ space, and the two-point dissipation term ϵ^* equals $\frac{1}{2}(\epsilon(\boldsymbol{\xi}_+) + \epsilon(\boldsymbol{\xi}_-))$.

At high-enough Reynolds numbers, the two-point viscous diffusion term D^* may be neglected. If we consider regions of turbulent flows where the integral scale $\mathcal{L}$ of the turbulent fluctuating velocity is smaller than or comparable to length scales characterizing spatial variations in $\mathbf{x}$ of mean flow statistics, then for high Reynolds numbers and $r < \mathcal{L}$,

$$\frac{\partial}{\partial t}<|\delta\mathbf{u}|^2> + \mathbf{U}(\mathbf{x})\cdot\boldsymbol{\nabla}_{\mathbf{x}}<|\delta\mathbf{u}|^2> + \boldsymbol{\nabla}_{\mathbf{r}}\cdot<\delta\mathbf{u}|\delta\mathbf{u}|^2> = \nu\boldsymbol{\nabla}^2_r<|\delta u|^2> - 4\epsilon. \tag{3}$$

Laizet et al. (2013) and P. Valente & J.C. Vassilicos (submitted manuscript) obtained a sufficient condition for the diffusion term $\nu\boldsymbol{\nabla}^2_{\mathbf{r}}<|\delta u|^2>$ to be negligible compared to 4ϵ and therefore drop out so as to be left with

$$\frac{\partial}{\partial t}<|\delta\mathbf{u}|^2> + \mathbf{U}(\mathbf{x})\cdot\boldsymbol{\nabla}_{\mathbf{x}}<|\delta\mathbf{u}|^2> + \boldsymbol{\nabla}_{\mathbf{r}}\cdot<\delta\mathbf{u}|\delta\mathbf{u}|^2> = -4\epsilon. \tag{4}$$

This sufficient condition is $r \gg \lambda$, where $\lambda^2 \equiv \nu\mathcal{U}^2/\epsilon$ (i.e., λ is effectively the Taylor microscale). In small-scale isotropic turbulence, Goto & Vassilicos (2009) proved under mild assumptions that λ is proportional to the average distance between stagnation points of the fluctuating velocity field. Hence, the fluctuating velocity is much rougher at scales larger than λ than at scales smaller than λ. Equation 4 therefore describes the rough range of the locally homogeneous velocity field, that is, the range of length scales r between λ (for roughness) and $\mathcal{L}$ (for local homogeneity in the appropriate conditions).

The key equilibrium assumption made by Kolmogorov (1941b) is that the small-scale motions ($r \ll \mathcal{L}$) evolve very quickly compared to the timescale of the overall turbulence evolution and are therefore in statistical equilibrium [i.e., $\partial/(\partial t)<|\delta\mathbf{u}|^2> + \mathbf{U}(\mathbf{x})\cdot\boldsymbol{\nabla}_{\mathbf{x}}<|\delta\mathbf{u}|^2> \approx 0$]. The equilibrium cascade then follows in the form $\boldsymbol{\nabla}_{\mathbf{r}}\cdot<\delta\mathbf{u}|\delta\mathbf{u}|^2> \approx -4\epsilon$. Nie & Tanveer (1999) (see also Duchon & Robert 2000, Eyink 2003) introduced the procedure of integrating both sides over a sphere of radius $|\mathbf{r}| = r$, which, using the Gauss divergence theorem, yields

$$\int \hat{\mathbf{r}}\cdot<\delta\mathbf{u}|\delta\mathbf{u}|^2>\, d\Omega \approx -\frac{16\pi}{3}\epsilon r, \tag{5}$$

where $d\Omega$ is the differential of the solid angle in $\mathbf{r}$ space and $\hat{\mathbf{r}} \equiv \mathbf{r}/r$.

This may be seen as summarizing the modern mathematical treatment and resulting expression of the Richardson-Kolmogorov cascade for equilibrium turbulence. The spherically averaged

interscale energy flux in physical space is negative, which means that the cascade is from large to small scales because turbulence velocity differences are being compressed (i.e., transported to smaller scales). The self-similarity of the cascade is also evident in this expression as the rate of energy across scales is determined by ϵ, regardless of the scale r in the appropriate range. This self-similarity is the basis for the dimensional analysis leading to the celebrated $E(k) \sim \epsilon^2 k^{-5/3}$ scaling of the turbulence energy spectrum $E(k)$ (e.g., see Pope 2000). Finally, to quote Pope (2000), this mathematical expression "of the cascade indicates that ϵ scales as $\mathcal{U}^3/\mathcal{L}$ independent of ν (at the high Reynolds numbers being considered)." Indeed, for $r \sim \mathcal{L}$, one expects $\int \hat{\mathbf{r}} \cdot <\delta\mathbf{u}|\delta\mathbf{u}|^2> d\Omega \sim \mathcal{U}^3$, which, from Equation 5, implies the equilibrium dissipation law

$$\epsilon = C_\epsilon \mathcal{U}^3/\mathcal{L}, \tag{6}$$

with C_ϵ = const. independent of the Reynolds number at high-enough Reynolds numbers. The clear weakness of this derivation is that Equation 5 holds for $r \ll \mathcal{L}$, yet Equation 5 is used for $r \sim \mathcal{L}$. These two conditions on r are not necessarily incompatible if one can write $\int \hat{\mathbf{l}} \cdot <\delta\mathbf{u}|\delta\mathbf{u}|^2> d\Omega \sim \mathcal{U}^3$ for a scale smaller than $\mathcal{L}$ that is nevertheless a fixed fraction of $\mathcal{L}$.

Equation 6 and $\lambda^2 \equiv \nu\mathcal{U}^2/\epsilon$ imply that

$$\mathcal{L}/\lambda \sim C_\epsilon Re_\lambda, \tag{7}$$

where $Re_\lambda \equiv (\mathcal{U}\lambda)/\nu$ is a local Reynolds number dependent on the position in the flow as $\mathcal{U}$ and λ depend on $\mathbf{x}$. This relation demonstrates that $\mathcal{L} \gg \lambda$ if $Re_\lambda \gg 1$ and therefore that intermediate scales r at which $\lambda \ll r \ll \mathcal{L}$ do exist at high-enough Reynolds numbers. In fact, Equation 7 expresses a central idea of the Richardson-Kolmogorov cascade: the higher the Reynolds number, the higher the range of scales required for the turbulent energy to be dissipated. This follows from the Richardson-Kolmogorov cascade's indication (to use Pope's word) that C_ϵ = const. Below are a few facts that substantiate Tennekes & Lumley's (1972) statement that the dissipation relation given in Equation 6 with C_ϵ = const. "should not be passed over lightly. It is one of the cornerstone assumptions of turbulence theory." It is noted that Equation 6 with C_ϵ = const. is an assumption for Tennekes & Lumley (1972), and also for Frisch (1995) (see below), whereas Kolmogorov (1941a,b) saw it as a consequence of his equilibrium assumption. Either way, there is a cornerstone assumption here that should not be passed over lightly.

First, the turbulent eddy viscosity ν_t in one-point Reynolds-averaged Navier-Stokes models of turbulence (see Launder & Spalding 1972, Pope 2000) is estimated using $\nu_t \sim \mathcal{U}\mathcal{L}$ and Equation 6 with C_ϵ = const. : $\nu_t \sim C_\epsilon \mathcal{U}^4/\epsilon$. Second, two-point turbulence modeling such as large-eddy simulations (see Lesieur & Metais 1996, Meneveau & Katz 2000) relies on the Richardson-Kolmogorov equilibrium cascade, which indicates that Equation 6 holds with C_ϵ = const. Third, the number of degrees of freedom is usually estimated as $(\mathcal{L}/\eta)^3$, where $\eta = (\nu^3/\epsilon)^{1/4}$ is the Kolmogorov microscale. The equilibrium relation given in Equation 6 with C_ϵ = const. is crucial in determining that $(\mathcal{L}/\eta)^3 \sim Re_L^{9/4}$; Re_L is another local Reynolds number based on $\mathcal{U}$ and $\mathcal{L}$, both of which are dependent on $\mathbf{x}$. Relations such as $(\mathcal{L}/\eta)^3 \sim C_\epsilon^{3/4} Re_L^{9/4}$ are pivotal when choosing the resolution of computer simulations of turbulent flows. Finally, the equilibrium dissipation relation given in Equation 6 with C_ϵ = const. effectively determines the streamwise development of mean profiles of self-preserving turbulent free shear flows (Townsend 1976, George 1989).

3. EVIDENCE FOR $\epsilon \sim \mathcal{U}^3/\mathcal{L}$ IN THE 50 YEARS AFTER THE 1941 PAPERS OF KOLMOGOROV

The equilibrium dissipation law in Equation 6 with C_ϵ = const. was in fact first introduced by Taylor (1935) without much justification six years before Kolmogorov's 1941 papers.

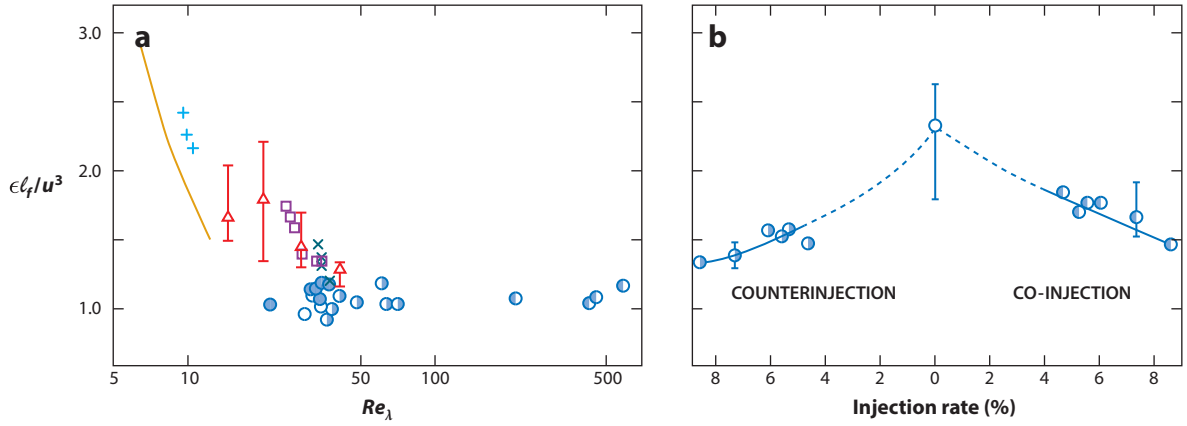

Figure 1

(*a*) C_ϵ as a function of Re_λ for a variety of biplane grid-turbulence data. In some cases, Re_λ is varied by varying the inlet Reynolds number; in others, Re_λ is varied by varying the position in the flow. The four highest Re_λ points on the plot are from Kistler & Vrebalovich (1966), who varied Re_λ by varying the inlet flow velocity while measuring at the same station. (*b*) C_ϵ as a function of the injection rate for the jet grids (early versions of a sort of active grid) of Gad-el-Hak & Corrsin (1974). Figure adapted with permission from Sreenivasan (1984). Copyright 1984, AIP Publishing LLC.

Interestingly, Taylor (1935) considered C_ϵ to be constant "for geometrically similar boundaries." This qualification points to another aspect of the constancy of C_ϵ besides its independence on the Reynolds number: its dependence or independence on boundary and inlet conditions.

Surprisingly perhaps, in the 50 years following Kolmogorov's 1941 publications, there seem to have been only a few attempts to obtain experimental evidence for C_ϵ = const. Batchelor (1953) compiled data for decaying turbulence in the lee of regular grids with various mesh sizes and for two different wind-tunnel speeds. In the words of Sreenivasan (1984), "he concluded that, in the so-called initial period of decay, the data are not generally inconsistent" with C_ϵ = const. Both Sreenivasan (1984) and Lumley (1992) mentioned the wide scatter in Batchelor's (1953) data and also Saffman's (1968) comment that a logarithmic or weak power-law dependence of C_ϵ on the Reynolds number cannot be ruled out by these data. To deal with this unsatisfactory state of affairs, Sreenivasan (1984) compiled all dissipation data available at the time from many different experiments and produced the well-known plot of C_ϵ versus Re_λ reproduced in **Figure 1*a***. This has proved an influential plot over the years as it suggests that C_ϵ tends to a constant value independent of Re_λ when Re_λ is larger than approximately 100 in turbulence generated by biplane square mesh grids. Sreenivasan (1984) also commented on data from other types of regular grids that suggest that C_ϵ may in fact take different asymptotic values for geometrically different inlet boundaries (to paraphrase Taylor 1935). Most relevant to some of the more recent developments on the topic (see Section 4) is a plot he based on the jet-grid data of Gad-el-Hak & Corrsin (1974) (**Figure 1*b***). This plot demonstrates the possibility of smoothly varying the value of C_ϵ by smoothly changing inlet conditions in the form of modified jet injection rates (see Gad-el-Hak & Corrsin 1974).

The data presented and discussed in Batchelor (1953) and Sreenivasan (1984) concern grid-generated turbulence. Antonia et al. (1980) obtained indirect laboratory support for Equation 6 with C_ϵ = const. in free shear flows, specifically one plane and three circular jets. These authors derived the power-law dependence of C_ϵ on the downstream distance from Equation 6 with C_ϵ = const., the requirements of mean-flow self-preservation, and the usual assumption that $\mathcal{L}$

is well represented by the jet width. They then showed that their data confirmed the predicted downstream variation of C_ϵ.

4. EVIDENCE FOR $\epsilon \sim \mathcal{U}^3/\mathcal{L}$ IN THE PAST 25 YEARS

There have been several developments since Lumley's (1992) review of the experimental evidence concerning C_ϵ: (*a*) Sreenivasan's (1995, 1998) updates and the advent of direct numerical simulations (DNS) capable of reaching Reynolds numbers large enough for meaningful tests of the constancy of C_ϵ in Equation 6, (*b*) a mathematically rigorous upper bound on dissipation that emulates Equation 6, (*c*) a new confined flow experiment originating from France, (*d*) contributions by Antonia and colleagues on the nonuniversality of the high–Reynolds number value of C_ϵ, (*e*) a relation between C_ϵ and a dimensionless number characterizing the number of large-scale eddies per integral scale, and (*f*) a distinction between decaying and forced homogeneous turbulence as far as C_ϵ is concerned and a new dissipation law for nonequilibrium turbulence.

Sreenivasan (1995) examined data from homogeneous shear flows and cylinder wakes. As in Batchelor (1953) and Sreenivasan (1984), the surrogates used for $\mathcal{U}$ and $\mathcal{L}$ in Equation 6 were the multiple of the root-mean-square streamwise turbulence fluctuating velocity $\sqrt{3/2}u_1'$ and the longitudinal integral length scale L_{11}. For homogeneous shear flows, Sreenivasan (1995) concluded that C_ϵ tends to a value independent of Re_λ as Re_λ increases above 100 but that C_ϵ is nevertheless weakly dependent on the shear. His turbulent wake data were obtained at a distance of 50 cylinder diameters from the wake-generating cylinder. There, C_ϵ proved to be independent of the inlet Reynolds number $Re_D = U_\infty D/\nu$, with U_∞ the fluid velocity upstream of the cylinder and D its diameter, for values of Re_D larger than approximately 1,000.

In Sreenivasan's (1998) update on C_ϵ, he examined data from DNS of homogeneous turbulence in a periodic box. This time C_ϵ was calculated from Equation 6 by taking $\mathcal{U}^2$ to be the total kinetic energy of the turbulence and $\mathcal{L}$ to be the integral length scale corresponding to the three-dimensional spectrum. With the exception of just three C_ϵ values that were from DNS of decaying turbulence, all other DNS of incompressible turbulence included a large-scale forcing in the Navier-Stokes equation to keep the turbulence at a statistically stationary state. The conclusion was that C_ϵ does indeed tend to a value independent of Re_λ for $Re_\lambda > 100$ but that this value may significantly differ for different large-scale forcings. Kaneda et al. (2003) carried out similar DNS of forced periodic turbulence at much higher Reynolds numbers and confirmed the Reynolds number independence of C_ϵ (calculated as in Sreenivasan 1998) up to $Re_\lambda \approx 1{,}200$.

Remaining in the realm of periodic forced Navier-Stokes turbulence, Doering & Foias (2002) rigorously proved from the incompressible Navier-Stokes equations that periodic and statistically stationary body-forced three-dimensional turbulence is such that $\epsilon \leq c_1 \nu \mathcal{U}/l^2 + c_2 \mathcal{U}^3/l$, where c_1 and c_2 are dimensionless Reynolds number–independent coefficients, and l is the longest length scale in the applied forcing assumed square-integrable. In the high–Reynolds number limit where $\nu \to 0$, this inequality is remarkably comparable to Equation 6. Rollin et al. (2011) showed that the high–Reynolds number value of the normalized dissipation rate depends on the shape of the low-wave-number forcing and that this shape dependence is captured by the upper-bound analysis. For a review of the three-dimensional Navier-Stokes problem and for references to other dissipation-rate bounds, the reader is referred to Doering (2009).

The DNS data in Sreenivasan (1998) and Kaneda et al. (2003) and the rigorous upper bound of Doering & Foias (2002) were obtained for statistically stationary forced incompressible Navier-Stokes turbulence in a periodic domain. A good and accessible account of the Richardson-Kolmogorov cascade and its related statistical laws in such a setting has been given by Frisch (1995), and it differs from the summary account given in Section 2 of the present review. Section 2

is concerned with the Richardson-Kolmogorov cascade for Equation 1, whereas Frisch (1995), Sreenivasan (1998), Kaneda et al. (2003), and Doering & Foias (2002) dealt with

$$\frac{\partial}{\partial t}\mathbf{u} + \mathbf{u}\cdot\boldsymbol{\nabla}_{\boldsymbol{\xi}}\mathbf{u} = -\boldsymbol{\nabla}_{\boldsymbol{\xi}} p + \nu\boldsymbol{\nabla}^2_{\boldsymbol{\xi}}\mathbf{u} + \mathbf{f}, \tag{8}$$

where $\mathbf{f}$ is a forcing term acting only at large scales. All these authors consider the situation in which $<\mathbf{f}\cdot\mathbf{u}> = \epsilon$, and Frisch (1995) derived Kolmogorov's famous 4/5 law, which is effectively the same as Equation 5 with the extra assumption of small-scale isotropy, by making the assumption that C_ϵ does not depend on the Reynolds number (see also Tchoufag et al. 2012 and Laizet et al. 2013 for related yet different approaches). Equation 6 with $C_\epsilon = \text{const.}$ is therefore a cornerstone assumption on which the Richardson-Kolmogorov cascade rests in the setting studied by Frisch (1995) and is not a consequence of the Richardson-Kolmogorov cascade as in Section 2. Another important difference is that all the terms in Equation 6 are independent of the spatial location in Frisch (1995), whereas $\mathcal{U}$ and $\mathcal{L}$ are not in the setting of Section 2.

An experimental development that has proven very influential over the past 25 years in various areas of investigation involving turbulent flow is the so-called French washing machine (Douady et al. 1991). This apparatus consists of a cylindrical tank with two coaxial counter-rotating stirrers at the top and bottom of the tank. Cadot et al. (1997) were motivated to use it to check the high–Reynolds number validity of Equation 6 with $C_\epsilon = \text{const.}$ by the absence of tests for this scaling in experiments in which statistically stationary turbulence is maintained in a closed container. To enhance the dissipation in the bulk of the fluid with respect to the boundary layers, they used rough (inertial) stirrers. Unlike previous measurements by Batchelor (1953) and Sreenivasan (1984, 1995), who used hot-wire anemometry to obtain local fluctuating velocities, Cadot et al. (1997) measured the global energy dissipation ϵ_G by measurements of the rate of mean temperature variations and also independently measured the total power P needed to drive the disks. They varied the global Reynolds number $\Omega R^2/\nu$, where Ω and R are the rotation frequency and radius of the disks, by varying Ω and by using different fluids with different viscosities. In all cases, they checked that P and ϵ_G closely balanced, and they plotted what effectively amounted to $C_{\epsilon G} \equiv (\epsilon_G R)/(\Omega R)^3$, which they found to be constant over more than three decades of $\Omega R^2/\nu$ (from 3×10^3 to 7×10^6). This experiment is perhaps the closest to the forced turbulence in a periodic box studied with DNS and mathematical analysis of the incompressible Navier-Stokes equations discussed above.

Antonia and collaborators addressed the issue, first briefly mentioned by Taylor (1935) and subsequently encountered in the data examined by Sreenivasan (1984, 1995, 1998), that C_ϵ depends on inlet/boundary/flow conditions. Antonia & Pearson (2000) made hot-wire measurements in two different two-dimensional wakes, one of a circular cylinder and one of a flat plate. They considered only one measurement station in each one of these wakes and varied the Reynolds number by varying the inlet flow velocity. Following Batchelor (1953) and Sreenivasan (1984, 1995), they calculated C_ϵ by replacing $\mathcal{U}$ with $\sqrt{3/2}u'_1$ and $\mathcal{L}$ with L_{11} in Equation 6. At an equal Reynolds number, Re_λ, they found different values of C_ϵ in different wakes, even though their measuring stations were deemed to be far from the wake generator, 54 and 62 diameters downstream of the cylinder and flat plate, respectively.

Burattini et al. (2005) extended the study to even more two-dimensional wakes, also looked at data from regular and active grid turbulence and homogeneous shear flow, and reported a wide variability of C_ϵ, between 0.5 and 2.5 for $Re_\lambda > 50$. They assigned this variability to a dependence on the flow configuration but not to a dependence on the Reynolds number. Boffetta & Romano (2002) took measurements at a streamwise distance of 40 jet diameters from a round jet exit and reported that C_ϵ does not vary with Re_λ over a wide range of Re_λ values.

By making use of the Rice theorem, which was brought into the study of turbulence by Liepmann (1949) and Liepmann & Robinson (1952), Mazellier & Vassilicos (2008) established a relation between C_ϵ and a dimensionless number C_s', which characterizes the large-scale flow topology of the turbulence. C_s' is effectively a number of large-scale eddies within an integral scale and is dependent on inlet/flow conditions. It is therefore not universal. Turbulence fluctuations being statistically self-similar, the small number of large scales is directly reflected in the large number of small scales. A way to quantify these numbers is to count zero crossings of both the signal itself and filtered versions of it. The average distance $\bar{l}$ between zero crossings is therefore strongly influenced by C_s' [Mazellier & Vassilicos (2008) gave a precise definition of C_s'], and by virtue of the Rice theorem, this average distance $\bar{l}$ is proportional to the Taylor microscale λ, itself directly related to ϵ. It then follows that $C_\epsilon \propto C_s'^3$ (see Mazellier & Vassilicos 2008 for detailed explanations). The strong flow/inlet dependence of C_ϵ already observed in previous investigations can therefore be quantified as a dependence on C_s', which is naturally dependent on flow/inlet conditions. This approach allowed Mazellier & Vassilicos (2008) to collapse 30 different C_ϵ values from seven different turbulent flows. Note that Mouri et al. (2012) and Thiesset et al. (2014) also found a significant dependence of C_ϵ on flow/inlet conditions, but they claimed that it was caused by the wrong choice of $\mathcal{L}$ to characterize the size of the large-scale energy-containing eddies. Mouri et al. (2012) collapsed 17 different C_ϵ values from three different turbulent flows by using the integral length scale of $u_1^2 - <u_1^2>$ instead of Batchelor's (1953) L_{11} choice of $\mathcal{L}$. Thiesset et al. (2014) collapsed 15 different such values (all measured in turbulent wakes at the same normalized distance from five different obstacles but with various inlet Reynolds numbers) by using a cross-over length scale that is intermediate between energy injection and maximum interscale energy transfer. The links between these two approaches and with the one based on the Rice theorem have not yet been investigated.

Goto & Vassilicos (2009) generalized the Rice theorem to stagnation points of a statistically homogeneous and isotropic incompressible fluctuating velocity field and showed that $\lambda = B\overline{l_s}$, where $\overline{l_s}$ is the average distance between stagnation points, and B is a dimensionless number with a very weak dependence on the Reynolds number caused by small-scale intermittency. In terms of a number C_s of large-scale stagnation points per integral scale [Goto & Vassilicos (2009) defined C_s in a precise way that generalizes C_s'], they showed that $C_\epsilon \sim C_s/B^3$. They then addressed the issue noted by Sreenivasan (1998) concerning DNS of statistically stationary turbulence in a periodic box, namely the dependence of C_ϵ on the large-scale forcing. They ran two different sets of DNS of such turbulence with two different types of large-scale forcing, which gave two different C_ϵ versus Re_λ curves (see **Figure 2*a***). However, when normalized by C_s/B^3 to plot $\tilde{C}_\epsilon = C_\epsilon B^3/C_s$ versus Re_λ, these two curves collapsed quite closely on each other (**Figure 2*b***). Hence, the dependence of C_ϵ on large-scale forcing can be quantified via the dependence of C_ϵ on the nonuniversal large-scale eddy structure of the turbulence. The generalized Rice theorem was critical in this development, and we note here that $\lambda = B\overline{l_s}$ has also been found to hold in DNS of turbulent channel flows in which, however, $\overline{l_s}$ was defined in planes parallel to the channel walls (see Dallas et al. 2009 in which this observation and its consequences on mean flow and dissipation profiles in the log layer are presented).

Bos et al. (2007) introduced a distinction between C_ϵ for homogeneous turbulence that is freely decaying (referred to as $C_\epsilon^{\text{decay}}$) and C_ϵ for homogeneous turbulence that is forced to remain at a statistically steady state (referred to as $C_\epsilon^{\text{forced}}$). This distinction arises because the energy input rate at the large scales balances the energy dissipation rate at the small scales at all times in the case of statistically stationary homogeneous turbulence, whereas such a balance can only be across times in the case of decaying homogeneous turbulence. In other words, in this latter case, the energy input rate at the large scales at a certain time balances the dissipation rate at the small

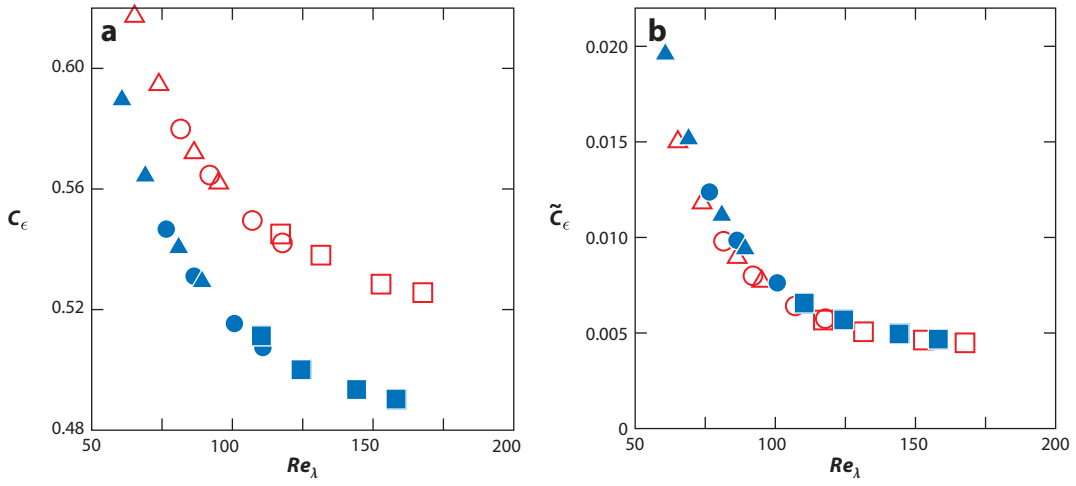

Figure 2

(*a*) C_ϵ as a function of Re_λ from direct numerical simulations of forced periodic statistically stationary turbulence. Closed and open symbols correspond to different large-scale forcing procedures. (*b*) $\tilde{C}_\epsilon = C_\epsilon B^3/C_s$ as a function of Re_λ for the same data. Figure adapted with permission from Goto & Vassilicos (2009). Copyright 2009, AIP Publishing LLC.

scales at a later time, with the difference between these two times being the time needed for the energy to cascade from large to small scales. These considerations expressed in equations lead to $C_\epsilon^{\text{decay}} \neq C_\epsilon^{\text{forced}}$. Bos et al. (2007) tested their ideas against DNS, large-eddy simulations, and the EDQNM (eddy-damped quasi-normal Markovian) spectral closure and found differences between $C_\epsilon^{\text{decay}}$ and $C_\epsilon^{\text{forced}}$, which add to the body of evidence suggesting that C_ϵ in Equation 6 is not universal in the sense that it depends on inlet/boundary conditions and the type of flow.

The standard attempt at generating decaying homogeneous turbulence in the laboratory involves a grid placed at the inlet of a wind tunnel's test section, the so-called grid turbulence. In such experiments, the role of time is played by the streamwise distance x from the grid, and the considerations of Bos et al. (2007) imply a value of $C_\epsilon^{\text{decay}}$ different from $C_\epsilon^{\text{forced}}$ but also invariant with x. In fact, the fundamental reason for this invariance with x is the Reynolds number independence of C_ϵ and that the local Reynolds number decays with increasing x. Several recent investigations discussed below have unveiled a type of decaying grid turbulence in which C_ϵ is not constant but in fact increases with x, even though the local Reynolds number does indeed decay with x.

5. THE NONEQUILIBRIUM DISSIPATION LAW

Grid-turbulence experiments in wind tunnels and water flumes using both hot-wire anemometry and particle image velocimetry have shown that a significant turbulence decay region exists in which $E_{11}(k_1) \sim k_1^{-5/3}$ over more than a decade of wave numbers, yet $C_\epsilon \sim Re_I^m/Re_L^n$ ($\neq$ const.), with $m \approx 1 \approx n$, $Re_I = (U_\infty L_b)/\nu$, and $Re_L = (u_1' L_{11})/\nu$ (Seoud & Vassilicos 2007, Mazellier & Vassilicos 2010, Valente & Vassilicos 2011, Gomes-Fernandes et al. 2012, Valente & Vassilicos 2012, Discetti et al. 2013, Nagata et al. 2013, Hearst & Lavoie 2014, Isaza et al. 2014, Valente & Vassilicos 2014). Re_I is a global or inlet Reynolds number based on the inlet flow speed U_∞ and a length scale L_b defined by the grid and does not depend on the local position in the flow. Re_L is a local Reynolds number that can, and does, differ from place to place in the flow.

Seoud & Vassilicos (2007) obtained the first evidence of a very different dissipation scaling in the decaying turbulence generated by some of the fractal square grids introduced by Hurst &

Vassilicos (2007). They recorded how $u_1'^2$, L_{11}, and ϵ vary as functions of the streamwise distance from the grid. They also found that, along the centerline, $C_\epsilon = \epsilon L_{11}/u_1'^3$ increases as Re_L decreases in such a way that $C_\epsilon \sim Re_L^{-1}$, even though the energy spectrum of the turbulence has a power-law range over more than a decade with an exponent very close, if not equal, to $-5/3$. In particular, they reported that L_{11}/λ remains constant as Re_L and Re_λ decay, which follows from Equation 7 and $C_\epsilon \sim Re_L^{-1}$. As mentioned in Section 2, the Richardson-Kolmogorov cascade is such that the range of length scales required for the turbulent energy to dissipate increases with increasing Reynolds number. This is not the case in the region of the flow that Seoud & Vassilicos (2007) investigated.

Mazellier & Vassilicos (2010) followed this work by noting that the actual constant value of L_{11}/λ is in fact an increasing function of the inlet Reynolds number and that the relation $C_\epsilon \sim Re_L^{-1}$ is increasingly clear with increasing Re_I (see **Figure 3**). They also introduced the wake interaction length scale x_* [revised and improved by Gomes-Fernandes et al. (2012)], which can be calculated from the geometry of the grid to predict the furthest point downstream (the one on the centerline with streamwise coordinate x_{peak}) beyond which the turbulence decays. As seen in **Figure 3**, the local Reynolds number increases from $x = 0$, where the grid is placed until approximately $x = 0.4x_*$, and then decays in the region $x > 0.4x_*$. The new dissipation behavior has been documented in a sizeable part of the decay region, $x > 0.4x_*$. To give an idea of the size, Gomes-Fernandes et al. (2012) confirmed that L_{11}/λ remains constant while Re_λ decays between $x = x_{peak}$ and $x = 3x_{peak}$ in a water channel of 0.6 m $\times$ 0.6 m cross-sectional area, where the fractal square grid used was such that $x_{peak} = 1.4$ m. The new dissipation behavior was therefore present between 1.4 m and 4.2 m from the grid in this channel. These authors were not able

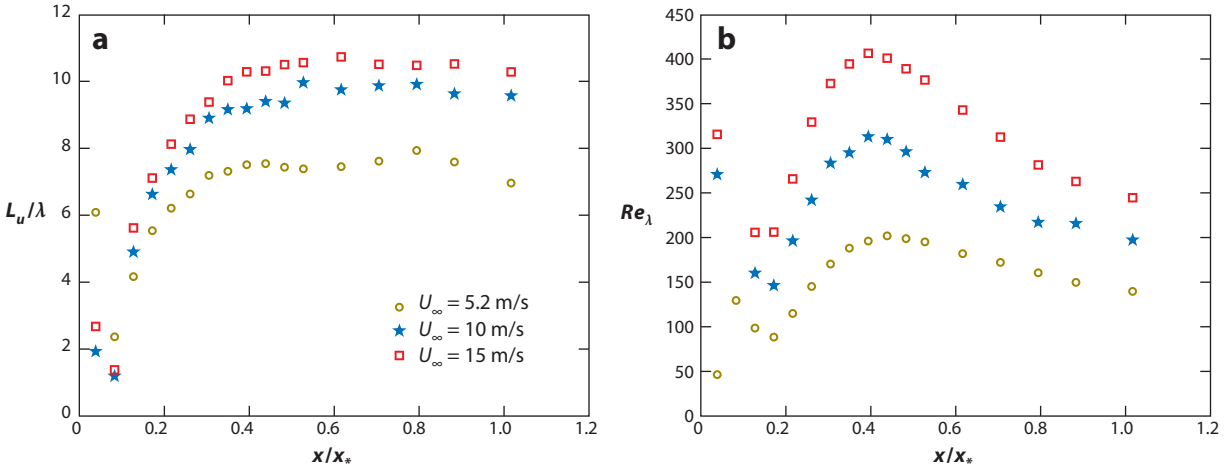

Figure 3

(*a*) Ratio of the longitudinal integral length scale L_{11} to the Taylor microscale λ as a function of the streamwise distance x from a turbulence-generating fractal square grid along the centerline. The distance x is normalized by the wake interaction length scale x_* introduced by Mazellier & Vassilicos (2010) and Gomes-Fernandes et al. (2012) as a predictor of the streamwise distance from the grid where the turbulence intensity peaks (around $x/x_* \approx 0.4$ in this case). Note the constancy of L_{11}/λ in the decay region $x/x_* > 0.4$ and the increasing constant value of L_{11}/λ with increasing inlet flow speed U_∞. (*b*) Re_λ as a function of x/x_* for the same grid and the same three different values of $U_\infty = 5.2$ m/s, 10 m/s, and 15 m/s. Figure adapted with permission from Mazellier & Vassilicos (2010).

to make measurements further downstream to determine the length of this region with unusual dissipation scaling.

Various profiles of one-point statistics have been extensively documented in the lee of fractal square grids (specifically high–thickness ratio, low-blockage, space-filling fractal square grids; see references below for these qualifications), and they have been reported by Hurst & Vassilicos (2007), Seoud & Vassilicos (2007), Mazellier & Vassilicos (2010), Valente & Vassilicos (2011), Nagata et al. (2013), and Discetti et al. (2013). The salient conclusions of these homogeneity investigations are that the turbulence is highly inhomogeneous and non-Gaussian in the production region close to the grid (i.e., $x < x_{\text{peak}}$) and then only weakly inhomogeneous (if not approximately homogeneous) and close to Gaussian in the decay region ($x > x_{\text{peak}}$) around the centerline, except for third-order moments, meaning that there is nonnegligible transverse energy and pressure transport. The isotropy/anisotropy characteristics in the decay region are broadly similar to those of regular grids. The streamwise extent over which the new dissipation scaling is reported around the centerline extends over a number of eddy turnover times, and the timescales of the energy-containing eddies are significantly smaller than the inverse mean flow gradients.

Valente & Vassilicos (2012) applied the wake interaction length scale to the design of two regular grids with unusually low blockage and a small number of meshes but with a value of x_{peak} larger than that of usual regular grids and comparable to that of previously used fractal square grids in the same wind-tunnel test section. This allowed a fair comparison between regular grid and fractal square grid turbulence in the same range of x/x_{peak} values for which the new dissipation scaling has been observed for fractal square grids. They concluded that their unusual regular grids display the same dissipation scaling in the decay region as the fractal square grids (i.e., $C_\epsilon = \epsilon L_{11}/u_1'^3$ increases while Re_L decreases so that $C_\epsilon \sim Re_L^{-1}$ and so that L_{11}/λ remains constant while Re_L decays). Again, as with fractal square grids, this behavior is accompanied by a very well-defined $-5/3$ turbulence energy spectrum, even though the Richardson-Kolmogorov cascade as we know it does not imply such a Reynolds number dependence on C_ϵ, nor does it imply a constant ratio of scales as the local Reynolds number decays.

Valente & Vassilicos (2012) also used a fractal square grid and a usual regular grid for two purposes: (*a*) to confirm and quantify Mazellier & Vassilicos's (2010) observation that the constant value of L_{11}/λ increases with global/inlet Reynolds number Re_I [Mazellier & Vassilicos (2010) had actually noted that this length-scale ratio is proportional to the square root of an inlet Reynolds number in all canonical free shear flows] and (*b*) to take advantage of the usual regular grid's small value of x_{peak} to explore how far downstream the new dissipation scalings hold in multiples of x_{peak}. Their measurements showed that $C_\epsilon \sim Re_I^m/Re_L^n$, with $m \approx 1 \approx n$ and L_b in $Re_I = (U_\infty L_b)/\nu$ being the largest mesh size on the grid (which is the actual mesh size in the case of regular grids). In the case of their usual regular grid, this new dissipation law was found to hold in $x_{\text{peak}} < x < 5x_{\text{peak}}$, with C_ϵ adopting a constant value at $x > 5x_{\text{peak}}$ (see **Figure 4*a***). Subsequently, these findings were confirmed by Isaza et al. (2014) with a usual regular grid of their own and by Hearst & Lavoie (2014) with a grid made of many repetitions of a fractal square grid so as to bring the value of x_{peak} down and probe a very wide range of x/x_{peak} in fractal-generated decaying turbulence (see **Figure 4*b***). Valente & Vassilicos (2014) surveyed various turbulent profiles in the decay region of various fractal and regular grids and showed that the new dissipation scaling is present irrespective of significant inhomogeneity and anisotropy differences between their grids. They also verified that this new dissipation scaling is not an artifact of anisotropy by trying different transverse and longitudinal surrogates for $\mathcal{U}$ and $\mathcal{L}$.

Section 2 ends with a reminder that the equilibrium dissipation relation given in Equation 6 with $C_\epsilon = \text{const.}$ effectively determines the streamwise development of mean profiles of self-preserving turbulent free shear flows (Townsend 1976, George 1989). In such flows, $\mathcal{U}$ scales

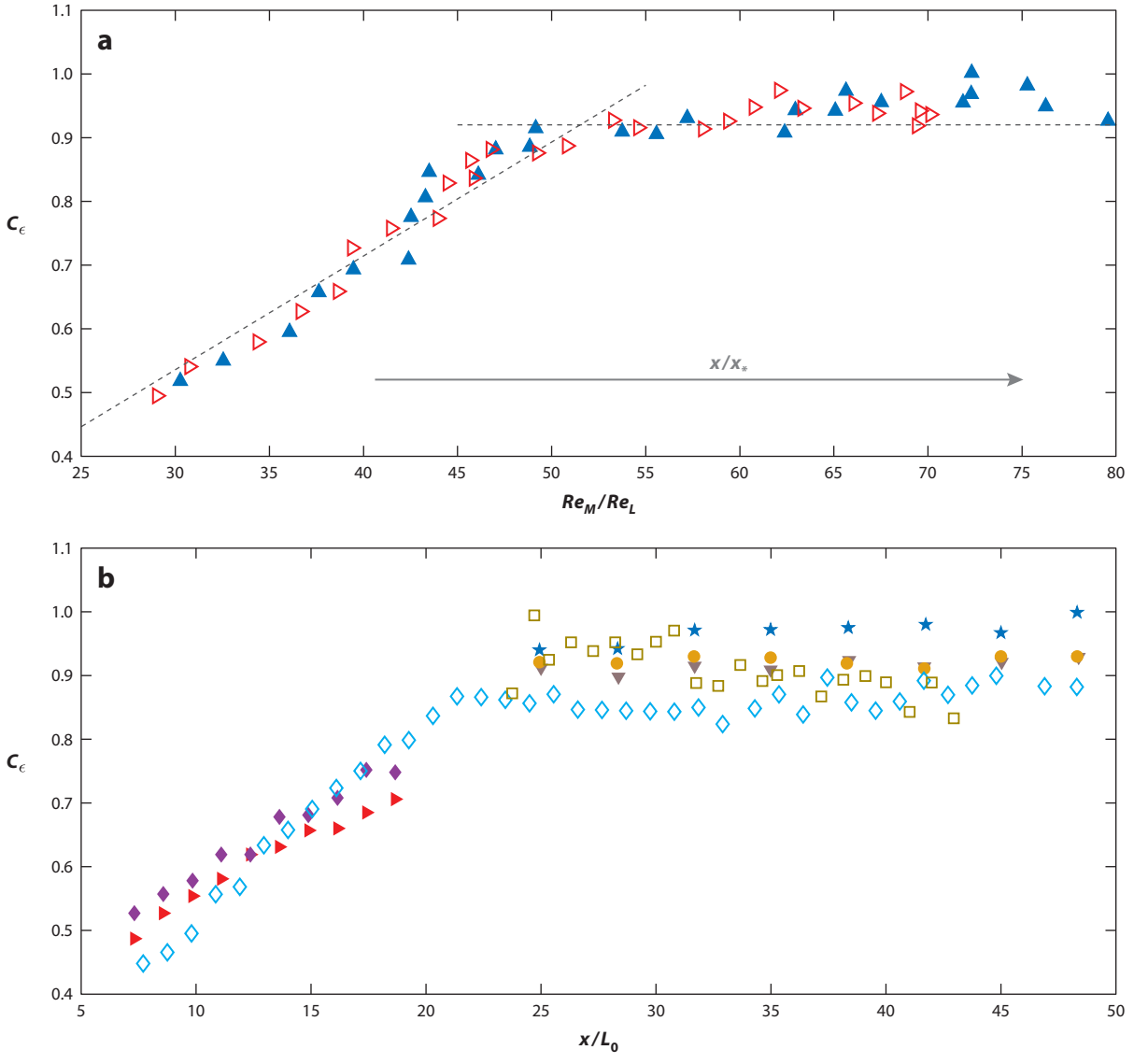

Figure 4

(*a*) C_ϵ versus Re_I/Re_L for a regular grid in which $Re_I = Re_M = U_\infty M/\nu$ as L_b is taken to be the mesh size M. Different symbols correspond to different values of Re_I. The streamwise distance from the grid is indicated in the plot and increases with increasing Re_I/Re_L. The sudden change from $C_\epsilon \sim Re_I/Re_L$ to $C_\epsilon \approx$ const. occurs at $x \approx 5x_{\text{peak}}$. Panel *a* adapted with permission from Valente & Vassilicos (2012). (*b*) C_ϵ versus x/L_0 for a square-fractal-element grid, where L_0 is the size of each square fractal element on the grid. The open symbols are for two different values of the inlet flow speed U_∞, and the closed symbols are data from Valente & Vassilicos (2011) for a regular grid and a fractal square grid at different values of U_∞. Panel *b* adapted from Hearst & Lavoie (2014) with permission from Cambridge University Press.

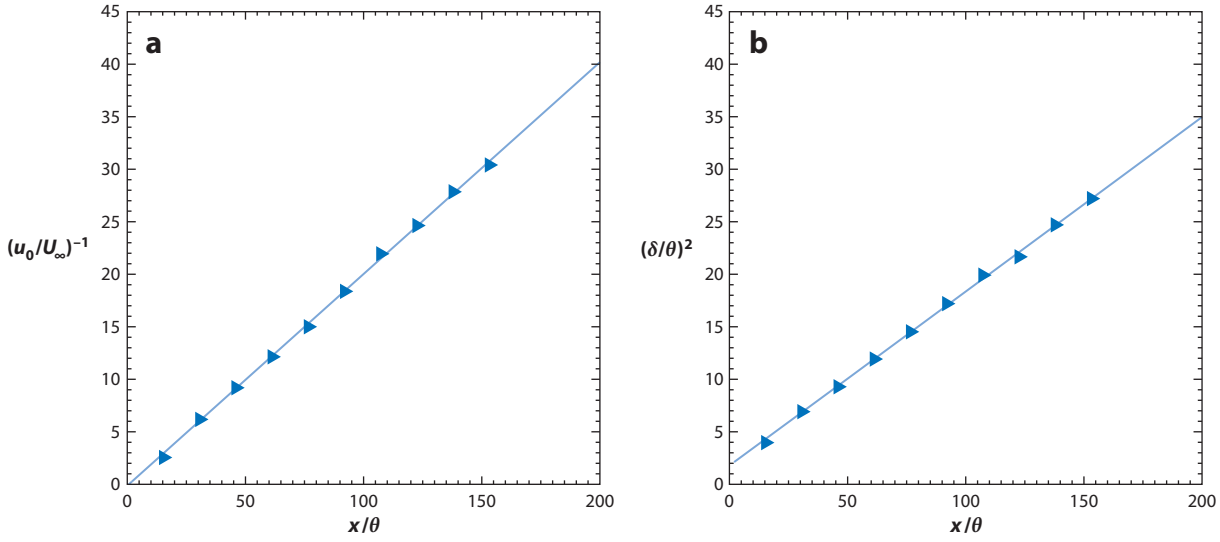

Figure 5

Plots corresponding to the turbulent axisymmetric and self-preserving wake of a plate with an irregular periphery: (*a*) $(u_0/U_\infty)^{-1}$ versus x/θ and (*b*) $(\delta/\theta)^2$ versus x/θ, where u_0 is the centerline mean velocity deficit, U_∞ is the constant upstream flow velocity, δ is the wake width, θ is the constant momentum thickness, and x is the streamwise distance from the wake-generating plate. Note that the linear dependencies on x (over the x range considered) are in agreement with $u_0/U_\infty \sim ((x - x_0)/\theta)^{-1}$ and $\delta/\theta \sim ((x - x_0)/\theta)^{1/2}$, which follow from the nonequilibrium dissipation scalings. Figure adapted with permission from Nedic et al. (2013).

with the centerline mean velocity deficit u_0, and the integral scale is taken to be proportional to the wake width δ. The Richardson-Kolmogorov cascade scaling $C_\epsilon = \text{const.}$ then implies $u_0/U_\infty \sim ((x - x_0)/\theta)^{-2/3}$ and $\delta/\theta \sim ((x - x_0)/\theta)^{1/3}$ for turbulent axisymmetric wakes, where U_∞ is the constant upstream flow velocity, and θ is the constant momentum thickness (see Townsend 1976, George 1989). Nedic et al. (2013) used the new dissipation scaling $C_\epsilon \sim Re_I^m/Re_L^n$ with $m = n = 1$ to derive its corresponding turbulent axisymmetric wake laws and found the very different scalings $u_0/U_\infty \sim ((x - x_0)/\theta)^{-1}$ and $\delta/\theta \sim ((x - x_0)/\theta)^{1/2}$. They then carried out wind-tunnel tests of axisymmetric wakes generated by plates with irregular peripheries placed normal to an incoming free stream and found that these new wake laws are present and very well defined in a downstream streamwise range between approximately $5\sqrt{A}$ and at least $50\sqrt{A}$, where A is the area of the plate (see **Figure 5**). The turbulence decays in this streamwise wake region, and one may expect a transition further downstream to the usual wake laws that stem from the equilibrium dissipation scaling $C_\epsilon = \text{const.}$

Some of the authors of the aforementioned papers referred to the new dissipation scaling $C_\epsilon \sim Re_I^m/Re_L^n$, with $m \approx 1 \approx n$, as a nonequilibrium turbulence dissipation law because it violates the Richardson-Kolmogorov cascade's suggestion that $C_\epsilon = \text{const.}$ and also appears to hold in various turbulent flows. It may be surprising to find the same dissipation law in different nonequilibrium decay regions of different turbulent flows. Actually, the exact values of n and m, even if close to 1, remain to be investigated, including the possibility that there may be some variations from flow to flow.

Concerning the nonequilibrium qualification of this new dissipation scaling, there are really three assumptions leading to Equation 6 with $C_\epsilon = \text{const.}$ in nonstationary turbulence (see Section 2). The major ones are local homogeneity and Kolmogorov's equilibrium hypothesis, but the third one (see Section 2) is the extrapolation of the equilibrium cascade relation given in

Equation 5 to $r \sim \mathcal{L}$. [Kolmogorov (1941b) actually made such an assumption too.] One cannot rule out the possibility that, in the region where the nonequilibrium dissipation law holds, the assumption at fault is in fact this third one. If that is the case, then this would also be an equilibrium failure, although not necessarily over the entire range of scales, only at the high end of it. Hence, the nonequilibrium qualification remains meaningful. Furthermore, if the equilibrium hypothesis and Equation 5 remain valid but only at much smaller values of r, then the nonequilibrium dissipation law would imply that the spherically averaged interscale energy flux strongly depends on the inlet Reynolds number, which violates the universality aspect of the Richardson-Kolmogorov cascade in a rather uniquely dramatic and explicit way. Either way, the nonequilibrium scaling signifies that the interscale energy transfers do not add up to a classical Richardson-Kolmogorov cascade in the region where this law is observed. If there is a cascade of sorts, and there most probably is, it is of a different type.

6. CONCLUSION AND DISCUSSION

There is a difference between forced statistically stationary turbulence in a periodic or closed box, on the one hand, and time/space-varying turbulence, in particular decaying turbulence, on the other. The DNS results reported by Sreenivasan (1998) and Kaneda et al. (2003), the inequality derived from the Navier-Stokes equation by Doering & Foias (2002), and the closed-container experiments of Cadot et al. (1997) lend strong support to Equation 6 with $C_\epsilon = \text{const.}$ in the context of forced statistically stationary turbulence in a box. In fact, in all these cases, $\mathcal{U}$ and $\mathcal{L}$ are independent of both space and time.

The situation appears to differ when the turbulence is decaying, both in a self-preserving axisymmetric turbulent wake and in decaying grid-generated turbulence apparently irrespective of the grid. As soon as the turbulence starts decaying along the streamwise direction in these flows, the normalized dissipation coefficient C_ϵ is found to be growing while the local Reynolds numbers Re_L and Re_λ are decreasing. This behavior is not the one suggested by the Richardson-Kolmogorov cascade, even though the energy spectra exhibit their best $-5/3$ wave-number scalings over the widest wave-number range in this nonequilibrium decay region where $C_\epsilon \sim Re_I^m/Re_L^n$, with $m \approx 1 \approx n$. In the few cases in which it has been possible to go far enough downstream in terms of the relevant length scale (x_{peak}), a sudden transition is observed to $C_\epsilon = \text{const.}$ Still, this constancy is in terms of the streamwise distance x and local Reynolds number, not necessarily in terms of the inlet conditions. As Taylor (1935) seems to have expected and as a number of authors have shown, starting with Sreenivasan and Antonia and his colleagues, C_ϵ can take different Reynolds number–independent values for different inlet/boundary conditions and different types of flow. Recently, Thormann & Meneveau (2014) substantially added to this bank of nonuniversality evidence with their extensive study of turbulence generated by various types of active fractal grids, which showed that C_ϵ differs for different inlet conditions. In doing so, they introduced new types of turbulent flows that will help future research developments.

It is essential for the observation of the nonequilibrium dissipation scaling to conduct experiments in which values of C_ϵ are recorded by varying both the global/inlet Reynolds number Re_I and the streamwise measurement location so as to vary the local Reynolds numbers Re_L and Re_λ without varying Re_I. Kistler & Vrebalovich (1966) obtained the four highest Re_λ data points in **Figure 1*a***** by measuring at one single point in the flow and varying the inlet Reynolds number Re_I only. Such measurements would return a value of C_ϵ that is more or less independent of the Reynolds number, irrespective of the position of the measuring station with respect to x_{peak}, either because C_ϵ is indeed constant or because $C_\epsilon \sim Re_I^m/Re_L^n$, with $m \approx 1 \approx n$, and Re_L increases linearly with Re_I. Without these four high–Reynolds number data points, **Figure 1*a*** is left with

only one data point at an Re_λ larger than 100 and is therefore much less, if at all, conclusive as to the constancy of C_ϵ. The importance of varying Re_I and Re_L independently for conclusive statements on C_ϵ has only surfaced in the past eight or so years.

One might be tempted to dismiss the new nonequilibrium dissipation scaling as a transient in space, even though it is, of course, not a transient in time in the flows in which it has been recorded. The nonequilibrium decay region is a well-defined, permanently present region in the lee of various turbulent flows that may not extend all the way downstream to the ultimate region where the flow may cease to be turbulent in a spectral sense (at least it is not known to extend so far in any flow to date). More to the point, this well-defined, permanently present region has similar, if not the same, dissipation scaling laws in a variety of turbulent flows and can therefore not be dismissed as unworthy of study. In some cases, the transition from this nonequilibrium decay region to a further downstream decay region where C_ϵ is independent of the local Reynolds number has been detected. The Kolmogorov $-5/3$ wave-number scaling of the spectrum in the decay region is at its clearest over the widest range of wave numbers in the nonequilibrium region where the local Reynolds number is higher than it is further downstream, yet the Richardson-Kolmogorov cascade does not seem to be the cascade or interscale energy transfer mechanism at work. In fact, Laizet et al. (2013) and Gomes-Fernandes et al. (2014a,b) have traced the existence of well-defined Kolmogorov $-5/3$ spectra to the highly inhomogeneous and non-Gaussian production region very close to the turbulence-generating grid (upstream of the entire decay region) where, according to Gomes-Fernandes et al.'s (2014b) particle image velocimetry analysis of the nonhomogeneous nonisotropic Kármán-Howarth-Monin equation (Equation 2), the cascade is inverse along an axis at a small angle to the streamwise direction and forward in the transverse direction. This combined forward-inverse cascade is definitely not a characteristic of the Richardson-Kolmogorov cascade, yet it appears in conjunction with a $-5/3$ streamwise energy spectrum. Power-law energy spectra with exponents close to $-5/3$ have also been reported in a cylinder wake within 1 cylinder diameter from the cylinder (Braza et al. 2006). Of course, it will be important in the future to carefully check the relation between the frequency and wave-number domains in such close-proximity flow regions.

Along with the production region, the nonequilibrium region is not only important fundamentally, it can also be expected to matter in many industrial, engineering, and environmental contexts, far more than the very far region beyond it. Nedic et al. (2013) recorded nonequilibrium wake scalings up to a distance of $50\sqrt{A}$, where A is the area of the wake-generating plate (see Section 5). This is a very long way downstream for many practical purposes, and new approaches will need to be developed to model the turbulence there. We are reminded of the quotation from Lumley (1992) at the start of this review: "What part of modeling is in serious need of work? Foremost, I would say, is the mechanism that sets the level of dissipation in a turbulent flow, particularly in changing circumstances."

The changing circumstances can be gradual, perhaps caused by no more than gradual turbulence decay, or sudden, as at the point downstream at which the turbulence suddenly transits from $C_\epsilon \sim Re_I^m/Re_L^n$, with $m \approx 1 \approx n$, to $C_\epsilon = \text{const.}$ (see **Figure 4**). There are several length scales that are beginning to surface in importance, such as x_{peak} and the wake interaction length scale that aims to predict x_{peak} in grid-generated turbulence. The point at which the aforementioned sudden change occurs is a multiple of x_{peak}, perhaps $5x_{\text{peak}}$ as in one of the regular grid experiments of Valente & Vassilicos (2012). An important question involves understanding the physical nature of this sudden change and the scalings of the point downstream where it happens. Related are similar questions for axisymmetric self-preserving turbulent wakes: What is the length scale at which the nonequilibrium scalings of the wake transit to the usual scalings, and what causes this sudden high to less high Reynolds number transition? The practical relevance and applications of

nonequilibrium turbulence depend quite critically on these length scales and our ability to predict them from the geometry of inlet/boundary conditions. Investigations similar to that of Nedic et al. (2013) are now waiting to be made for other self-preserving turbulent free shear flows, such as jets, mixing layers, and other types of wakes, and similar questions may arise there too.

Recently, George (2014) advanced an argument suggesting that the Kolmogorov energy spectrum scaling $E(k) \sim \epsilon^{2/3} k^{-5/3}$ is inconsistent with the Kolmogorov local equilibrium assumption for decaying homogeneous turbulence (the critical assumption that allows one to go from Equation 4 to Equation 5 and obtain the Richardson-Kolmogorov cascade in nonstationary turbulence). His claim may be consistent with the unusual dissipation scalings in the nonequilibrium decay region downstream of regular and fractal grids where the turbulence energy spectrum has a well-defined $-5/3$ range. Further downstream where $C_\epsilon = \text{const.}$, George's (2014) claim (if correct) would imply either an absence of a Kolmogorov spectral range or, if such a range does exist [including both the $\epsilon^{2/3}$ and $k^{-5/3}$ scalings of $E(k)$], a situation in which $C_\epsilon = \text{const.}$ is not the result of a high–Reynolds number Richardson-Kolmogorov cascade. Such far-downstream measurements are difficult because they require high local Reynolds numbers in a far region where the local Reynolds number has decayed. More work in this direction is required for the future, which may or may not produce evidence of a clear $C_\epsilon = \text{const.}$ with respect to variations in both Re_I and x in the far field combined with a clear well-defined Kolmogorov scaling range in the energy spectrum. The active fractal grids of Thormann & Meneveau (2014) may prove useful here, particularly if the integral length scales returned by some of them are well defined.

Concerning the nonequilibrium decay region, self-preserving, single-scale spectral theories based on the spectral equivalent of the Kármán-Howarth-Monin equation (the so-called Lin equation), such as those of George (1992) and George & Wang (2009), violate Kolmogorov's equilibrium assumption and lead to $C_\epsilon \sim 1/Re_L$ but not to $C_\epsilon \sim Re_I/Re_L$, even though they are not necessarily inconsistent with the latter. Mazellier & Vassilicos (2010) compared fractal-generated turbulence data from the nonequilibrium decay region with such theories (see also Valente & Vassilicos 2011) and found good agreement but also found that the very small scales can nevertheless be collapsed with the Kolmogorov microscale η, a feature that poses a challenge to these theories. Following these developments, there is now an obvious and pressing need to directly address the nature of the turbulence cascade and its scalings in nonequilibrium and in $C_\epsilon = \text{const.}$ regions by studying interscale energy fluxes and balances in the nonhomogeneous, nonisotropic Kármán-Howarth-Monin equation (Equation 2) or its spectral equivalent, if it can be meaningfully defined. Bai et al. (2013) and P. Valente & J.C. Vassilicos (submitted manuscript) have started addressing this need. Bai et al. (2013) found that the measured energy flux is strongly dependent on the scale at the turbulent near-wake flow downstream of a fractal tree-like object; P. Valente & J.C. Vassilicos (submitted manuscript) found an important contribution of the unsteady term in Equation 2 albeit at relatively low Reynolds numbers in the nonequilibrium and $C_\epsilon = \text{const.}$ regions of regular grids. Their experiment also confirms McComb et al.'s (2010) DNS result that the peak inertial flux scales as $\mathcal{U}^3/\mathcal{L}$ at relatively low Reynolds numbers.

FUTURE ISSUES

1. Other turbulent flows need to be explored for nonequilibrium non-Richardson-Kolmogorov cascades, such as DNS of periodic decaying or more generally statistically unsteady turbulence at high Reynolds numbers following McComb et al. (2010), whose DNS was of low–Reynolds number periodic and decaying turbulence; DNS of periodic and decaying superfluid turbulence consisting of a normal viscous fluid interacting with

a quantum inviscid vortex tangle via a mutual friction force (see Barenghi et al. 2014); and other boundary-free turbulent shear flows, such as various jets and mixing layers and other types of wakes, particularly those in which the local Reynolds number varies with the downstream distance. Finally, what happens in wall turbulence? Could similar nonequilibrium dissipation regions be present there too?

2. What causes the sudden transition from $C_\epsilon \sim Re_I^m/Re_L^n$, with $m \approx 1 \approx n$, to $C_\epsilon = \text{const.}$ (see **Figure 4**), and what is the downstream distance where this happens? How can this downstream distance be estimated in terms of the geometry of the turbulence generator and inlet Reynolds number? Is this distance related to the one at which one might expect a transition from the nonequilibrium wake laws of **Figure 5** to the classical wake laws? What about other boundary-free shear flows? How close to the grid is the demarcation between production and decay regions in turbulence generated by jet grids (Gad-el-Hak & Corrsin 1974), active grids (Makita 1991), and active fractal grids (Thormann & Meneveau 2014), and is there also a nonequilibrium decay region in such turbulent flows? How can one use the spatiotemporal properties of such grids to estimate downstream length scales demarcating different regions?
3. What is "the mechanism that sets the level of dissipation in a turbulent flow, particularly in changing circumstances"? This is a question that remains unanswered since Lumley (1992) asked it a quarter of a century ago, except that we now have a dissipation scaling for nonequilibrium turbulence. How can we explain $C_\epsilon \sim Re_I^m/Re_L^n$, with $m \approx 1 \approx n$, and what are the properties of the interscale transfers and turbulence cascade that come with it?

DISCLOSURE STATEMENT

The author is not aware of any biases that might be perceived as affecting the objectivity of this review.

ACKNOWLEDGMENTS

I am grateful to Professor Charles Doering and Dr. Oliver Buxton for the helpful comments they made on an early version of this article. I would also like to acknowledge the important contributions of Drs. Susumu Goto, Sylvain Laizet, and Nicolas Mazellier and of my PhD students Drs. Vassilis Dallas, Rafael Gomes-Fernandes, Daryl Hurst, Jovan Nedic, Richard Seoud, and Pedro Valente in the research that we carried out together over the past 12 years or so.

LITERATURE CITED

Antonia RA, Pearson BR. 2000. Effect of initial conditions on the mean energy dissipation rate and the scaling exponent. *Phys. Rev. E* 62:8086–90

Antonia RA, Satyaprakash BR, Hussain AKMF. 1980. Measurements of dissipation rate and some other characteristics of turbulent plane and circular jets. *Phys. Fluids* 23:695–700

Bai K, Meneveau C, Katz J. 2013. Experimental study of spectral energy fluxes in turbulence generated by a fractal, tree-like object. *Phys. Fluids* 25:110810

Barenghi CF, L'vov VS, Roche PE. 2014. Experimental, numerical, and analytical velocity spectra in turbulent quantum fluid. *Proc. Natl. Acad. Sci. USA* 111:4683–90

Batchelor GK. 1953. *The Theory of Homogeneous Turbulence*. Cambridge, UK: Cambridge Univ. Press

Boffetta G, Romano GP. 2002. Structure functions and energy dissipation dependence on Reynolds number. *Phys. Fluids* 14:3453–58

Bos WJT, Shao L, Bertoglio JP. 2007. Spectral imbalance and the normalized dissipation rate of turbulence. *Phys. Fluids* 19:045101

Braza M, Perrin R, Hoarau Y. 2006. Turbulence properties in the cylinder wake at high Reynolds numbers. *J. Fluids Struct.* 22:757–71

Burattini P, Lavoie P, Antonia RA. 2005. On the normalized turbulent energy dissipation rate. *Phys. Fluids* 17:098103

Cadot O, Couder Y, Daerr A, Douady S, Tsinober A. 1997. Energy injection in closed turbulent flows: stirring through boundary layers versus inertial stirring. *Phys. Rev. E* 56:427–33

Dallas V, Vassilicos JC, Hewitt GF. 2009. Stagnation point von Kármán coefficient. *Phys. Rev. E* 80:046306

Danaila L, Krawczynski JF, Thiesset F, Renou B. 2012. Yaglom-like equation in axisymmetric anisotropic turbulence. *Physica D* 241:216–23

Discetti S, Ziskin IB, Astarita T, Adrian RJ, Prestridge KP. 2013. PIV measurements of anisotropy and inhomogeneity in decaying fractal generated turbulence. *Fluid Dyn. Res.* 45:061401

Doering CR. 2009. The 3D Navier-Stokes problem. *Annu. Rev. Fluid Mech.* 41:109–28

Doering CR, Foias C. 2002. Energy dissipation in body-forced turbulence. *J. Fluid Mech.* 467:289–306

Douady S, Couder Y, Brachet ME. 1991. Direct observation of the intermittency of intense vorticity filaments in turbulence. *Phys. Rev. Lett.* 67:983–86

Duchon J, Robert R. 2000. Inertial energy dissipation for weak solutions of incompressible Euler and Navier-Stokes equations. *Nonlinearity* 13:249–55

Eyink GL. 2003. Local 4/5-law and energy dissipation anomaly in turbulence. *Nonlinearity* 17:137–45

Frisch U. 1995. *Turbulence: The Legacy of A.N. Kolmogorov*. Cambridge, UK: Cambridge Univ. Press

Gad-el-Hak M, Corrsin S. 1974. Measurements of the nearly isotropic turbulence behind a uniform jet grid. *J. Fluid Mech.* 62:115–43

George WK. 1989. The self-preservation of turbulent flows and its relation to initial conditions and coherent structures. In *Advances in Turbulence*, ed. WK George, R Arndt, pp. 39–73. New York: Hemisphere

George WK. 1992. The decay of homogeneous isotropic turbulence. *Phys. Fluids A* 4:1492–509

George WK. 2014. Reconsidering the 'local equilibrium' hypothesis for small scale turbulence. In *Turbulence Colloquium Marseille 2011: Fundamental Problems of Turbulence, 50 Years After the Marseille 1961 Conference*, ed. M Farge, HK Moffatt, K Schneider. Les Ulis, Fr.: EDP Sci. In press

George WK, Wang H. 2009. The exponential decay of homogeneous turbulence. *Phys. Fluids* 21:025108

Gomes-Fernandes R, Ganapathisubramani B, Vassilicos JC. 2012. Particle image velocimetry study of fractal-generated turbulence. *J. Fluid Mech.* 711:306–36

Gomes-Fernandes R, Ganapathisubramani B, Vassilicos JC. 2014a. Evolution of the velocity-gradient tensor invariants in a spatially developing flow. *J. Fluid Mech.* 756:252–92

Gomes-Fernandes R, Ganapathisubramani B, Vassilicos JC. 2014b. The energy cascade in a non-homogeneous non-isotropic turbulence. *J. Fluid Mech.* Submitted manuscript

Goto S, Vassilicos JC. 2009. The dissipation rate is not universal and depends on the internal stagnation point structure. *Phys. Fluids* 21:035104

Hearst RJ, Lavoie P. 2014. Decay of turbulence generated by a square fractal-element grid. *J. Fluid Mech.* 741:567–84

Hill RJ. 2002. Exact second-order structure-function relationships. *J. Fluid Mech.* 468:317–26

Hurst D, Vassilicos JC. 2007. Scalings and decay of fractal-generated turbulence. *Phys. Fluids* 19:035103

Isaza JC, Salazar R, Warhaft Z. 2014. On grid-generated turbulence in the near and far field regions. *J. Fluid Mech.* 753:402–26

Kaneda Y, Ishihara T, Yokohama M, Itakura K, Uno A. 2003. Energy dissipation rate and energy spectrum in high resolution direct numerical simulations of turbulence in a periodic box. *Phys. Fluids* 15:L21–24

Kistler AL, Vrebalovich T. 1966. Grid turbulence at high Reynolds numbers. *J. Fluid Mech.* 26:37–47

Kolmogorov AN. 1941a. Dissipation of energy in locally isotropic turbulence. *Dokl. Akad. Nauk. SSSR* 32:16–18

Kolmogorov AN. 1941b. On degeneration (decay) of isotropic turbulence in an incompressible viscous fluid. *Dokl. Akad. Nauk. SSSR* 31:538–40

Kolmogorov AN. 1941c. The local structure of turbulence in incompressible viscous fluid for very large Reynolds numbers. *Dokl. Akad. Nauk. SSSR* 30:301–5
Laizet S, Vassilicos JC, Cambon C. 2013. Interscale energy transfer in decaying turbulence and vorticity-strain rate dynamics in grid-generated turbulence. *Fluid Dyn. Res.* 45:061408
Launder BE, Spalding DB. 1972. *Mathematical Models of Turbulence*. London: Academic
Lesieur M, Metais O. 1996. New trends in large-eddy simulations of turbulence. *Annu. Rev. Fluid Mech.* 28:45–82
Liepmann HW. 1949. Die anwendung eines satzes uber die nullstellen stochstischer functionen auf turbulenzmessungen. *Helv. Phys. Acta* 22:119–24
Liepmann HW, Robinson MS. 1952. *Counting methods and equipment for mean-value measurements in turbulence research*. NACA Tech. Note 3037, Natl. Advis. Comm. Aeronaut.
Lumley JL. 1992. Some comments on turbulence. *Phys. Fluids A* 4:201–11
Makita H. 1991. Realization of a large-scale turbulence field in a small wind tunnel. *Fluid Dyn. Res.* 8:53–64
Marati N, Casciola CM, Piva R. 2004. Energy cascade and spatial fluxes in wall turbulence. *J. Fluid Mech.* 521:191–215
Mazellier N, Vassilicos JC. 2008. The turbulence dissipation constant is not universal because of its universal dependence on large-scale flow topology. *Phys. Fluids* 20:015101
Mazellier N, Vassilicos JC. 2010. Turbulence without Richardson-Kolmogorov cascade. *Phys. Fluids* 22: 075101
McComb WD, Berera A, Salewski M, Yoffe S. 2010. Taylor's (1935) dissipation surrogate reinterpreted. *Phys. Fluids* 22:061704
Meneveau C, Katz J. 2000. Scale-invariance and turbulence models for large-eddy simulation. *Annu. Rev. Fluid Mech.* 232:1–32
Mouri H, Hori A, Kawashima Y, Hashimoto K. 2012. Large-scale length that determines the mean rate of energy dissipation in turbulence. *Phys. Rev. E* 86:026309
Nagata K, Sakai Y, Inaba T, Suzuki H, Terashima O, Suzuki H. 2013. Turbulence structure and turbulence kinetic energy transport in multiscale/fractal-generated turbulence. *Phys. Fluids* 25:065102
Nedic J, Vassilicos JC, Ganapathisubramani B. 2013. Axisymmetric turbulent wakes with new non-equilibrium similarity scalings. *Phys. Rev. Lett.* 111:144503
Nie Q, Tanveer S. 1999. A note on third-order structure functions in turbulence. *Proc. R. Soc. Lond. A* 455:1615–35
Pope SB. 2000. *Turbulent Flows*. Cambridge, UK: Cambridge Univ. Press
Richardson LF. 1922. *Weather Prediction by Numerical Process*. Cambridge, UK: Cambridge Univ. Press
Rollin B, Dubief Y, Doering CR. 2011. Variations on Kolmogorov flow: turbulent energy dissipation and mean flow profiles. *J. Fluid Mech.* 670:204–13
Saffman PG. 1968. Lectures on homogeneous turbulence. In *Topics in Nonlinear Physics*, ed. N Zabuski, pp. 485–614. Berlin: Springer-Verlag
Seoud RE, Vassilicos JC. 2007. Dissipation and decay of fractal-generated turbulence. *Phys. Fluids* 19:105108
Sreenivasan KR. 1984. On the scaling of the turbulence energy dissipation rate. *Phys. Fluids* 27:1048–59
Sreenivasan KR. 1995. The energy dissipation in turbulent shear flows. In *Symposium on Developments in Fluid Dynamics and Aerospace Engineering*, ed. SM Deshpande, A Prabhu, KR Sreenivasan, PR Viswanath, pp. 159–90. Bangalore: Interline
Sreenivasan KR. 1998. An update on the energy dissipation rate in isotropic turbulence. *Phys. Fluids* 10:528–29
Taylor GI. 1935. Statistical theory of turbulence. *Proc. R. Soc. Lond. A* 151:421–44
Tchoufag J, Sagaut P, Cambon C. 2012. Spectral approach to finite Reynolds number effects on Kolmogorov's 4/5 law in isotropic turbulence. *Phys. Fluids* 24:015107
Tennekes H, Lumley JL. 1972. *A First Course in Turbulence*. Cambridge, MA: MIT Press
Thiesset F, Antonia RA, Danaila L. 2013. Scale-by-scale turbulent energy budget in the intermediate wake of two-dimensional generators. *Phys. Fluids* 25:115105
Thormann A, Meneveau C. 2014. Decay of homogeneous nearly isotropic turbulence behind active fractal grids. *Phys. Fluids* 26:025112

Townsend AA. 1976. *The Structure of Turbulent Shear Flow*. Cambridge, UK: Cambridge Univ. Press
Valente P, Vassilicos JC. 2011. The decay of turbulence generated by a class of multi-scale grids. *J. Fluid Mech.* 687:300–40
Valente P, Vassilicos JC. 2012. Universal dissipation scaling for nonequilibrium turbulence. *Phys. Rev. Lett.* 108:214503
Valente P, Vassilicos JC. 2014. The non-equilibrium region of grid-generated decaying turbulence. *J. Fluid Mech.* 744:5–37

Annual Review of
Fluid Mechanics

Volume 47, 2015

Contents

Indexes

Errata

An online log of corrections to *Annual Review of Fluid Mechanics* articles may be found at http://www.annualreviews.org/errata/fluid